

MR Imaging Measures of Intracranial Atherosclerosis in a Population-based Study¹

Ye Qiao, PhD
 Eliseo Guallar, MD, DrPH
 Fareed K. Suri, MD
 Li Liu, MS
 Yiyi Zhang, PhD
 Zeeshan Anwar, MD
 Saeedeh Mirbagheri, MD
 YuanYuan Joyce Xie, MD
 Nariman Nezami, MD
 Jarunee Intrapiromkul, MD
 Shuqian Zhang MD
 Alvaro Alonso MD PhD
 Haitao Chu, PhD
 David Couper, PhD
 Bruce A. Wasserman, MD

¹From The Russell H. Morgan Department of Radiology and Radiological Science, Johns Hopkins Hospital, 367 East Park Building, 600 N Wolfe St, Baltimore, MD 21287 (Y.Q., L.L., Z.A., S.M., Y.J.X., N.N., J.I., S.Z., B.A.W.); Department of Epidemiology, Johns Hopkins Bloomberg School of Public Health, Baltimore, Md (E.G., Y.Z.); Department of Neurology, University of Minnesota, Minneapolis, Minn (F.K.S.); School of Public Health, University of Minnesota, Minneapolis, Minn (A.A., H.C.); School of Public Health, University of North Carolina, Chapel Hill, NC (D.C.). Received May 21, 2015; revision requested July 27; revision received November 9; accepted December 8; final version accepted January 7, 2016. **Address correspondence to** B.A.W. (e-mail: bwasser@jhmi.edu).

This study was supported by National Institutes of Health grants R01HL105930, R01HL105626, and K99HL106232. The ARIC Study is part of a collaborative study supported by contracts HHSN268201100005C, HHSN268201100006C, HHSN268201100007C, HHSN268201100008C, HHSN268201100009C, HHSN268201100010C, HHSN268201100011C, and HHSN268201100012C from the National Heart, Lung, and Blood Institute (NHLBI). Neurocognitive data are collected by U01 HL096812, HL096814, HL096899, HL096902, HL096917 from the NHLBI and the National Institute of Neurologic Disorders and Stroke, and with previous brain MR imaging examinations funded by R01-HL70825 from the NHLBI

© RSNA, 2016

Purpose:

To implement a magnetic resonance (MR) imaging protocol to measure intracranial atherosclerotic disease (ICAD) in a population-based multicenter study and report examination and reader reliability of these MR imaging measurements and descriptive statistics representative of the general population.

Materials and Methods:

This prospective study was approved by the institutional review boards and compliant with HIPAA. Atherosclerosis Risk in Communities (ARIC) study participants ($n = 1980$) underwent brain MR imaging from 2011 to 2013 at four ARIC sites. Imaging included three-dimensional black-blood MR imaging and time-of-flight MR angiography. One hundred two participants returned for repeat MR imaging to estimate examination and reader variability. Plaque presence according to vessel segment was recorded. Quantitative measurements included lumen size and degree of stenosis, wall and/or plaque thickness, area and volume, and normalized wall index for each vessel segment. Reliability was assessed with percentage agreement, κ statistics, and intraclass correlation coefficients.

Results:

Of the 1980 participants, 1755 (mean age, 77.6 years; 1026 women [59%]; 1234 white [70%]) completed examinations with adequate to excellent image quality. The weighted ICAD prevalence was 34.4% (637 of 1755 participants) and was higher in men than women (38.5% [302 of 729 participants] vs 31.7% [335 of 1026 participants], respectively; $P = .012$) and in African Americans compared with whites (41.1% [215 of 518 participants] vs 32.4% [422 of 1234 participants], respectively; $P = .002$). Percentage agreement of plaque identification per participant was 87.0% (interreader estimate), 89.2% (intrareader estimate), and 89.9% (examination estimate). Examination and reader reliability ranged from fair to good (κ , 0.50–0.78) for plaque presence and from good to excellent (intraclass correlation coefficient, 0.69–0.99) for quantitative vessel wall measurements.

Conclusion:

Vessel wall MR imaging is a reliable tool for identifying and measuring ICAD and provided insight into ICAD distribution across a U.S. community-based population.

© RSNA, 2016

Online supplemental material is available for this article.

Intracranial atherosclerotic disease (ICAD) is a major cause of ischemic stroke worldwide (1,2) and an important public health concern in the United States and globally. The prevalence of ICAD and associated luminal narrowing in the general population, however, is unknown because of the lack of appropriate diagnostic tools with which to depict intracranial vessel walls in population studies (3). Angiography, the traditional tool for diagnosing ICAD (4), may underestimate ICAD because vessels are capable of compensatory dilatation (remodeling) to accommodate plaque formation without luminal narrowing, particularly early on (5).

Vessel wall magnetic resonance (MR) imaging is an effective method with which to measure wall thickness and identify pathologic features of extracranial vessels (6). Although imaging intracranial vessel walls presents a greater technical challenge given the small size and tortuosity of these vessels, the recent development of a new three-dimensional (3D) black-blood MR imaging technique has made it possible to identify and characterize thickened intracranial vessel walls. This technique has gained

much attention and is beginning to be implemented for clinical applications (7–9) even though its reliability remains unknown, with only repeat observer reproducibility estimates reported in small numbers of participants (7). The reliability of extracranial carotid wall thickness measurements at MR imaging depends on the thickness of the wall relative to image resolution (10), with inadequate spatial resolution leading to grossly exaggerated thickness measurements (11). The thinner walls of intracranial arteries challenge the limits of image resolution even further, highlighting the importance of understanding measurement reliability for these examinations.

The Atherosclerosis Risk in Communities (ARIC) study is a prospective population-based study conducted in four U.S. communities (12). A recent neurocognitive substudy (the ARIC–Neurocognitive Study [NCS]) examined 6538 participants who participated in the ARIC study to investigate risk factors and vascular markers of cognitive impairment, with approximately 2000 of the participants undergoing brain MR imaging. As part of ARIC–NCS, we sought to implement an MR imaging protocol to measure ICAD in a population-based multicenter study and report examination and reader reliability of these MR imaging measurements and descriptive statistics representative of the general population.

Materials and Methods

Study Design and Study Participants

The ARIC study was designed to study cardiovascular disease in middle-aged (ages 45–64 years) African American

and white participants recruited from 1987 to 1989 to represent four U.S. communities (Forsyth County, NC; Jackson, Miss; suburban Minneapolis, Minn; and Washington County, Md) (12). For ARIC–NCS, ARIC participants were recruited for brain MR imaging from 2011 to 2013 to investigate associations of vascular risk factors with cognitive impairment and brain parenchymal changes observable at MR imaging. Of the participants, 1980 (1187 women [60.0%], 1410 white [71.2%], 564 African American [28.5%], six other [0.3%]) were selected for this MR examination by using a probability sampling plan to oversample participants with evidence of cognitive impairment and who had previously undergone brain MR imaging in the ARIC study. We added MR imaging sequences to identify plaque and measure the intracranial vessel wall, lumen area, and plaque when present. The study was approved by the institutional review board at each field site, and all participants provided written informed consent.

MR Imaging Protocol

ARIC–NCS brain MR imaging was performed with the following 3.0-T units,



Advances in Knowledge

- Three-dimensional vessel wall MR imaging offered good to excellent reliability (intraclass correlation coefficient, 0.69–0.99) for quantitative vessel wall measurements and fair to good reliability (κ , 0.50–0.78) in the identification of intracranial atherosclerotic disease (ICAD).
- At least one ICAD lesion was seen in 637 of 1755 participants (34.4% prevalence weighted to represent a U.S. community-based population), and the weighted prevalence was higher in men than in women (38.5% [302 of 729 participants] vs 31.7% [335 of 1026 participants], respectively; $P = .012$) and in African Americans compared with whites (41.1% [215 of 518 participants] vs 32.4% [422 of 1234 participants], respectively; $P = .002$).

Implications for Patient Care

- Vessel wall MR imaging is a reliable imaging tool for identifying ICAD and measuring plaque burden, which are important markers of stroke risk.
- Our study stratified ICAD frequency according to age, sex, and race, enabling the identification of individuals who might benefit most from screening.

Published online before print

10.1148/radiol.2016151124 Content codes:  

Radiology 2016; 280:860–868

Abbreviations:

ARIC = Atherosclerosis Risk in Communities
 ICAD = Intracranial atherosclerotic disease
 NCS = Neurocognitive Study
 QC = quality control
 3D = three-dimensional
 TOF = time of flight
 2D = two-dimensional

Author contributions:

Guarantors of integrity of entire study, Y.Q., F.K.S., B.A.W.; study concepts/study design or data acquisition or data analysis/interpretation, all authors; manuscript drafting or manuscript revision for important intellectual content, all authors; manuscript final version approval, all authors; agrees to ensure any questions related to the work are appropriately resolved, all authors; literature research, Y.Q., B.A.W.; clinical studies, F.K.S., N.N., J.I., S.Z., B.A.W.; statistical analysis, E.G., L.L., Y.Z., Z.A., H.C., B.A.W.; and manuscript editing, Y.Q., E.G., L.L., Y.Z., Z.A., N.N., J.I., A.A., D.C., B.A.W.

Conflicts of interest are listed at the end of this article.

all of which were manufactured by Siemens (Erlangen, Germany): Forsyth County, Magnetom Skyra, 32-channel head coil; Jackson, Magnetom Skyra, 20-channel head coil; Minneapolis, Magnetom Trio, 12-channel head coil; and Washington County, Magnetom Verio, 12-channel head coil. Examinations were performed by 13 MR imaging technologists trained, tested, and certified by the MR imaging reading center after imaging 23 volunteers across the four sites. Total protocol time, including brain MR imaging sequences not used for vessel characterization, was approximately 45 minutes.

The vascular sequences were performed at the end of a standardized brain MR imaging protocol and consisted of 3D time-of-flight (TOF) MR angiography and 3D high-isotropic-resolution black-blood MR imaging (7,8). Three-dimensional TOF MR angiography was performed in a transverse plane through the circle of Willis, centered to include the distal vertebral artery segments inferiorly and the middle cerebral artery branches superiorly, with the following parameters: repetition time msec/echo time msec, 21/3.7; flip angle, 18°; field of view, 160 mm × 160 mm²; matrix, 320 × 320; acquired resolution, 0.50 × 0.50 mm²; section thickness, 0.55 mm; number of sections, 148 (Trio) or 152 (Verio and Skyra); and imaging time, approximately 5 minutes.

The 3D black-blood MR imaging volume was oriented in a coronal plane (64-mm-thick slab) to cover the major intracranial vessels as identified on the images from TOF MR angiography. The technical design of this sequence has been previously described (7). Briefly, it is a 3D turbo spin-echo acquisition that uses a variable flip angle refocusing control that was optimized to augment the vessel wall signal and enable a longer echo train length for more effective lumen signal suppression. The center of k-space is sampled at the beginning of the echo train to minimize T2 weighting, thereby darkening the signal of the surrounding cerebrospinal fluid.

Imaging parameters were as follows: 1800/34; turbo factor, 64; echo

spacing, 5.6 msec; parallel imaging (generalized autocalibrated partially parallel acquisition or GRAPPA) acceleration factor, 2 (right-left direction); field of view, 160 × 160 × 64 mm³; matrix, 320 × 320 × 128; acquired resolution, 0.5 × 0.5 × 0.5 mm³; number of sections, 128; number of signals acquired, 1.4; and acquisition time, 8.3 minutes. Contrast material was not administered.

Image Analysis

All MR images were analyzed by seven certified readers (Y.Q., Z.A., S.M., Y.J.X., N.N., J.I., and S.Z., with 10, 3, 5, 2, 2, 4, and 10 years of experience, respectively) at the MR imaging reading center without knowledge of the participant characteristics. The average training period was 3 months, during which the readers had to accurately analyze a series of challenging cases preselected to represent anticipated case scenarios.

Vascular MR images (TOF MR angiograms and black-blood MR images) were first reviewed for quality control (QC) scores that graded image quality and protocol adherence. Image quality was graded on the basis of three criteria (flow suppression, vessel wall delineation, and artifacts) by using a four-point scale (0, failure; 1, poor with some information; 2, adequate; 3, excellent). Protocol adherence was graded on the basis of deviations in parameter selection and slab positioning by using a three-point scale (0, failure; 1, adequate; 2, excellent). Images with adequate or excellent QC scores were analyzed. Images rated as poor or failed were excluded.

Qualitative analysis.—Qualitative analysis was performed by using a picture archiving and communication system workstation (Ultravizual; Ema-geon, Birmingham, Ala). Images from 3D black-blood MR imaging and 3D TOF MR angiography were coregistered and reconstructed in both short and long axes relative to the flow direction. Vascular territories were categorized as right and left internal carotid artery, right and left middle cerebral artery, right and left posterior cerebral artery, right and left anterior cerebral artery, basilar artery, and right and left

vertebral artery (Table E1 [online]). Atherosclerotic plaque was defined as eccentric wall thickening with or without luminal stenosis seen at MR angiography (8). Lumen patency was assessed at the site of wall thickening identified on black-blood MR images and compared with the corresponding location on the TOF MR angiogram. If no narrowing was identified on the TOF MR angiogram, the plaque was considered to have no detectable stenosis. The number of detectable plaques in each vascular territory was recorded. For each territory, the ordinal degree of narrowing (ie, no detectable stenosis, <50% stenosis, 51%–70% stenosis, 71%–99% stenosis, and occlusion) was recorded for the most stenotic plaque, which was measured on TOF MR angiograms by using criteria established in the Warfarin-Aspirin Symptomatic Intracranial Disease Trial (13).

Quantitative analysis.—Quantitative measurements included lumen size and stenosis measured at MR angiography and wall and/or plaque size measured at black-blood MR imaging. The lumen boundary was contoured on the MR angiogram by using nonuniform rational B-spline, or NURBS, surface modeling software (LAVA; Leiden University Medical Center, the Netherlands) (14) and coregistered with the black-blood MR image, which was used to generate outer wall contours also by means of NURBS modeling. Measurements of lumen size and stenosis were based on tubular model contours from MR angiography, and measurements of wall and/or plaque size were based on lumen and outer wall contours from a tubular model of the black-blood MR imaging segmentation (Fig 1).

Quantitative measurements were obtained at designated vessel segments (supraclinoid internal carotid artery, M1 of middle cerebral artery, A1 of anterior cerebral artery, proximal and distal basilar artery, and V4 of vertebral artery) over a fixed length for all participants and for the largest plaque identified for each vascular territory in the qualitative assessment (Table E2 [online], Fig E1 [online]). For each vessel segment and plaque, we recorded

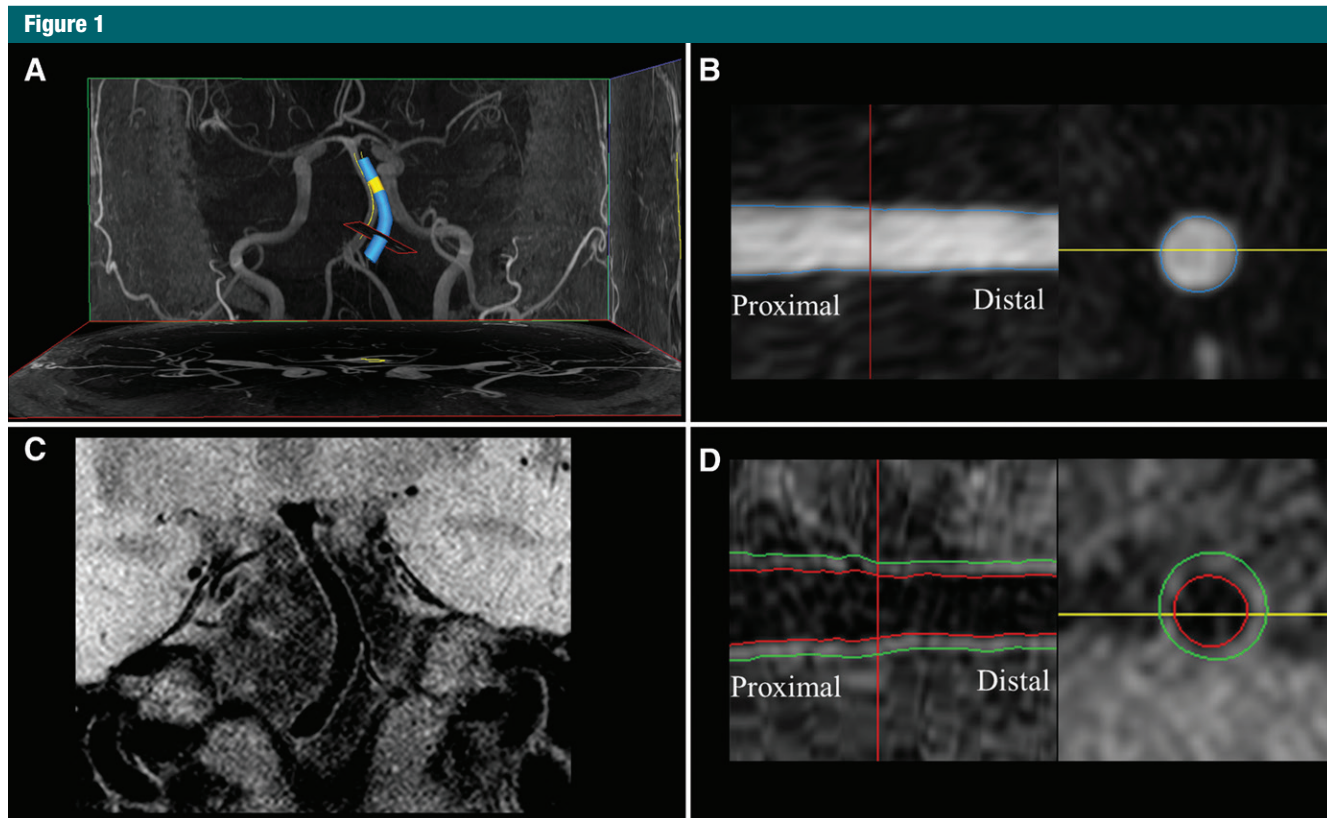


Figure 1: MR images of intracranial arteries in 79-year-old white man. *A*, Basilar artery lumen is contoured on MR angiogram with 3D nonuniform rational B-splines (or NURBS) modeling (LAVA software). *B*, Two-dimensional (2D) long-axis view shows that the contoured lumen is unfolded (left). *C*, *D*, Basilar artery segment identified on *C*, black-blood MR image is coregistered with MR angiogram lumen data and the wall contoured and unfolded in *D*, 2D long-axis view (left). Cross-sectional images are reconstructed to facilitate manually adjusting contours (*B* and *D*, right, corresponding to position of red line).

lumen size and degree of stenosis (both area- and diameter-based), wall and/or plaque thickness, area, volume, and normalized wall index (wall area/outer wall area).

Quality assurance.—After the MR imaging technologists underwent training and certification at the MR imaging reading center, feedback was regularly provided to MR imaging technologists for deviations in protocol adherence within 3 days of image acquisition. Image analysts were checked periodically by the principal investigator for errors in interpretation, with retraining when needed. Research Electronic Data Capture, or REDCap, software (version 5.12.2, Vanderbilt University, Nashville, Tenn) (15) was used to generate biweekly reports of analyst productivity, image quality, protocol adherence, and distributions of MR

imaging measurements. Alerts were generated for MR imaging measurements that exceeded expected biologic thresholds, and data were checked when indicated.

Reliability Study

We recruited 102 participants for repeat MR imaging to estimate reliability of both image acquisition and reading. Participants for repeated imaging were selected among those with MR images with adequate or excellent image quality showing at least one intracranial plaque. All repeated examinations and readings were assigned alternate identification numbers to ensure blinding of both the MR imaging technologists and the readers. The target between-examination interval was 13 weeks to minimize within-person biologic variation.

Only examination pairs with adequate or excellent QC scores at both visits were analyzed for reliability estimates. The complete set of repeat examinations was used to estimate qualitative reliability. To minimize the time-consuming effort required for quantitative analyses, we targeted a minimum of 20 examination pairs for quantitative reliability estimates, each including measurements for eight vessel segments and plaque. This target was needed to reliably estimate intraclass correlation coefficients of 0.7 or higher. Seven readers interpreted the repeat examinations. The target interval between readings by the same reader was at least 90 days to minimize recall bias. Repeat reading reliability estimates were based on 100 examination pairs for interreader estimates and 83 examination pairs for intrareader estimates,

whereas examination estimates were based on readers reading all available examination pairs.

Statistical Methods

All MR imaging data were collected and managed by using REDCap software (15). The data were then exported to Stata 12.1 (Stata Inc, College Station, Tex) for statistical analysis. We used Stata svy commands with sampling weights and strata to account for oversampling of participants with cognitive impairment in the ARIC-NCS MR imaging examination and provide estimates referable to the 6538 ARIC participants from whom MR imaging participants were recruited. Tests of equality of means and proportions across race and sex groups were based on regression analysis and Pearson χ^2 statistic, respectively, corrected for the survey design.

Reliability of categorical variables (eg, plaque presence and stenosis degree) was assessed by using percentage agreement and Cohen κ weighted for differences between stenosis categories (ie, 100%, 80%, 50%, and 0% agreement were assigned for reader differences of 0, 1, 2, and >2 grades, respectively).

Reliability of continuous variables was assessed by using intraclass correlation coefficients and coefficients of variation estimated from random effects models (10). Agreement between repeated examinations and repeated readings was assessed with Bland-Altman plots, and bias was examined by using paired t tests. Reliabilities of less than 0.4 were characterized as poor, 0.4–0.75 as fair to good, and greater than 0.75 as excellent (16). $P < .05$ was considered indicative of a statistically significant difference.

Results

Of the 1980 ARIC participants enrolled in the ARIC-NCS brain MR imaging study, 21 did not complete the vascular MR examinations (ie, both MR angiography and black-blood MR imaging) owing to imager malfunction ($n = 3$) or participant intolerance to MR imaging ($n = 18$). Of the 1959 completed

Table 1

Quantitative Intracranial Vascular MR Imaging Variables according to Race and Sex

Variable and Vessel	African American Participants		White Participants		P Value
	Men ($n = 184$)	Women ($n = 334$)	Men ($n = 545$)	Women ($n = 689$)	
Lumen area (mm²)					
MCA	3.72 (0.06)	3.35 (0.06)	4.00 (0.02)	3.35 (0.02)	<.001
ICA	7.62 (0.08)	6.97 (0.09)	8.35 (0.03)	7.51 (0.03)	<.001
ACA	2.19 (0.05)	1.90 (0.04)	2.56 (0.02)	2.19 (0.02)	<.001
BA	6.10 (0.07)	5.34 (0.06)	6.20 (0.03)	5.11 (0.02)	<.001
VA	5.34 (0.07)	4.62 (0.05)	5.66 (0.03)	4.37 (0.02)	<.001
Mean wall thickness (mm)					
MCA	1.03 (0.02)	1.04 (0.02)	1.02 (0.01)	1.02 (0.01)	.430
ICA	1.02 (0.02)	1.02 (0.02)	1.00 (0.01)	0.98 (0.01)	.404
ACA	1.07 (0.02)	1.09 (0.02)	1.05 (0.01)	1.04 (0.01)	.021
BA	0.99 (0.02)	0.97 (0.02)	0.96 (0.01)	0.93 (0.01)	<.001
VA	0.99 (0.02)	0.99 (0.02)	0.99 (0.01)	0.97 (0.01)	.030
Wall volume (mm³)					
MCA	71.1 (2.31)	65.7 (2.07)	63.3 (1.12)	59.4 (0.99)	<.001
ICA	78.6 (4.60)	74.0 (3.61)	75.1 (1.50)	67.7 (1.46)	<.001
ACA	64.7 (2.23)	60.0 (2.23)	60.9 (1.07)	54.8 (0.95)	<.001
BA	65.8 (1.95)	59.5 (1.72)	61.8 (0.86)	54.2 (0.74)	<.001
VA	78.9 (3.46)	74.3 (3.17)	73.3 (1.36)	64.2 (1.25)	<.001
Normalized wall index (%)					
MCA	66.5 (1.04)	68.8 (0.98)	66.1 (0.39)	68.4 (0.37)	<.001
ICA	56.4 (1.27)	57.8 (1.38)	55.7 (0.43)	57.1 (0.42)	<.001
ACA	74.4 (0.76)	77.1 (0.65)	73.4 (0.31)	74.8 (0.32)	<.001
BA	61.1 (1.09)	62.8 (1.08)	60.0 (0.41)	62.1 (0.40)	<.001
VA	62.3 (1.15)	64.2 (1.12)	62.5 (0.49)	65.7 (0.46)	<.001

Note.—All measurements except for wall volume are averaged over the fixed length for each vessel segment. Measurements are weighted to the ARIC participant recruitment pool ($n = 6538$). P values represent the difference among the four mean values with regression analysis adjusted for age and imaging sites, corrected for the survey design. Numbers in parentheses are standard errors. ACA = anterior cerebral artery, BA = basilar artery, ICA = internal carotid artery, MCA = middle cerebral artery, VA = vertebral artery.

examinations, 194 (9.9%) were excluded for failed or poor QC scores and 10 (0.5%) for misregistration between TOF and black-blood MR images. A complete set of qualitative and quantitative MR imaging measurements was available for 1755 participants (mean age, 77.6 years; 1026 women [58%]; 1234 white [70.3%]; 518 African American [29.5%]) who had examinations with adequate or excellent QC scores (Table E3 [online]). Image quality and protocol adherence scores were excellent for 66% and 95% of examinations, respectively.

Of the 1755 participants, 637 (36.3%) had at least one intracranial lesion (weighted prevalence to the entire

ARIC cohort, 34.4%). Weighted prevalence increased with age (26.4% [46 of 173 participants], 30.9% [178 of 554 participants]), 34.5% [185 of 517 participants], and 44.6% [228 of 517 participants] for participants 65–69, 70–74, 75–79, and 80 years or older, respectively; $P < .001$), and it was higher in men than in women (38.5% [302 of 729 participants] vs 31.7% [335 of 1026 participants], respectively; $P = .012$) and in African Americans compared with whites (41.1% [215 of 518 participants] vs 32.4% [422 of 1234 participants], respectively; $P = .002$). Quantitative MR imaging measurements grouped according to race and sex are shown in Table 1.

Table 2

Reliability Based on Repeat MR Examinations and Readings: Qualitative Variables

Artery and Variable	Interreader Estimate (<i>n</i> = 100)		Intrareader Estimate (<i>n</i> = 83)		Examination Estimate (<i>n</i> = 96)	
	Agreement (%)	κ	Agreement (%)	κ	Agreement (%)	κ
MCA						
Plaque presence	91.0	0.76 (0.58, 0.87)	90.4	0.78 (0.59, 0.88)	85.4	0.63 (0.45, 0.80)
Stenosis	94.9	0.67 (0.45, 0.73)	95.8	0.77 (0.64, 0.86)	93.4	0.59 (0.32, 0.74)
ACA						
Plaque presence	94.0	0.54 (0.22, 0.78)	94.0	0.58 (0.25, 0.81)	95.5	0.76 (0.47, 0.92)
Stenosis	96.0	0.53 (0.13, 0.80)	97.8	0.57 (0.41, 0.79)	98.2	0.71 (0.40, 0.82)
ICA						
Plaque presence	80.0	0.59 (0.41, 0.73)	75.9	0.50 (0.28, 0.66)	79.8	0.60 (0.38, 0.71)
Stenosis	88.9	0.47 (0.24, 0.54)	88.7	0.42 (0.30, 0.56)	84.3	0.57 (0.43, 0.71)
PCA						
Plaque presence	89.0	0.76 (0.60, 0.86)	90.4	0.77 (0.57, 0.88)	82.0	0.65 (0.48, 0.79)
Stenosis	94.2	0.74 (0.61, 0.80)	94.4	0.73 (0.56, 0.80)	91.3	0.58 (0.44, 0.67)
BA						
Plaque presence	90.0	0.68 (0.46, 0.82)	91.6	0.76 (0.54, 0.88)	91.0	0.68 (0.43, 0.80)
Stenosis	95.2	0.64 (0.37, 0.80)	95.8	0.73 (0.49, 0.87)	96.2	0.69 (0.55, 0.83)
VA						
Plaque presence	85.0	0.52 (0.30, 0.70)	88.0	0.67 (0.45, 0.82)	83.1	0.63 (0.43, 0.77)
Stenosis	90.7	0.56 (0.32, 0.82)	94.5	0.77 (0.55–0.94)	87.2	0.55 (0.33, 0.76)
Overall						
Plaque presence	87.0	0.59 (0.37, 0.75)	89.2	0.70 (0.48, 0.84)	89.9	0.68 (0.44, 0.82)
Stenosis	93.8	0.63 (0.50, 0.66)	94.4	0.68 (0.64, 0.75)	93.2	0.60 (0.52, 0.67)

Note.—Inter- and intrareader estimates were based on readers reading identical examinations (*n* = 100 and 83, respectively), whereas examination estimates were based on readers reading examination pairs (*n* = 96). Stenosis categories were as follows: no detectable stenosis, less than 50% stenosis, 51%–70% stenosis, 71%–99% stenosis, and occluded. Overall reliability is based on plaque presence per participant or stenosis per territory for all repeated examinations. For plaque presence, all standard errors of κ were approximately 0.1. For stenosis, standard errors of κ were approximately 0.07 for each vessel territory and 0.03 overall. Numbers in parentheses are the 95% confidence interval. ACA = anterior cerebral artery, BA = basilar artery, ICA = internal carotid artery, MCA = middle cerebral artery, PCA = posterior cerebral artery, VA = vertebral artery.

Of the 102 participants who underwent repeat MR imaging (mean age, 78.0 years; 49% women [50 of 102 participants]; 75% white [76 of 102 participants]), 96 had adequate or excellent QC scores at both visits. The median interval between repeat imaging was 14 weeks (interquartile range, 8.5–19 weeks) and that between repeat readings was 38.4 weeks (interquartile range, 35.6–44.8 weeks). Percentage agreement was 87.0% (interreader estimate), 89.2% (intrareader estimate), and 89.9% (examination estimate) for plaque identification and 93.8% (interreader estimate), 94.4% (intrareader estimate), and 93.2% (examination estimate) for ordinal stenosis (Table 2). Examination and reader reliability (κ value) ranged from fair to good for both plaque presence and ordinal stenosis. For plaque identification, reliability estimates showed little

difference between vessel segments. Ordinal stenosis reliability was lowest for the internal carotid artery, likely because of its tortuous course and frequent cavernous calcifications, which hinder luminal stenosis evaluation.

Examination and reader reliability (intraclass correlation coefficient) ranged from 0.66 to 0.99, with small measurement errors (coefficients of variation estimates) for lumen and wall size (Table 3). Inter- and intrareader estimates were based on readers reading 20 and 29 identical examinations, respectively (123 and 194 paired vessel segments, respectively), whereas examination estimates were based on readers reading 28 examination pairs (188 paired vessel segments). Coefficients of variation estimates for luminal stenosis were high because of the high frequency of segments with no

stenosis. Bland-Altman plots showed good agreement without a bias ($P > .05$) (Fig 2). Reliability estimates showed little difference by vessel location, except for the internal carotid artery, which showed the lowest reliability (mean wall thickness and normalized wall thickness estimates are shown in Table E4 [online]). Intrareader reliability was consistently higher than interreader and examination reliability.

Discussion

We have shown that 3D vessel wall MR imaging is a reliable tool for identifying and measuring ICAD. This technique revealed ICAD as highly prevalent in a U.S. community-based population and can potentially provide insight into identifying individuals who might benefit most from early intervention.

Table 3

Reliability Based on Repeat MR Examinations and Readings: Quantitative Variables

Variable	Interreader Estimate (n = 20)			Intrareader Estimate (n = 29)			Examination Estimate (n = 28)		
	CV	ICC	95% CI	CV	ICC	95% CI	CV	ICC	95% CI
Lumen area	0.28	0.89	0.80, 0.97	0.29	0.97	0.94, 0.99	0.33	0.97	0.93, 0.99
Lumen diameter	0.14	0.92	0.83, 0.98	0.15	0.98	0.95, 0.99	0.16	0.97	0.93, 0.99
Area-based stenosis	0.65	0.67	0.38, 0.90	0.61	0.67	0.48, 0.90	0.54	0.51	0.28, 0.75
Diameter-based stenosis	0.64	0.66	0.38, 0.90	0.59	0.65	0.45, 0.89	0.54	0.52	0.29, 0.75
Wall area	0.16	0.71	0.45, 0.94	0.21	0.83	0.64, 0.93	0.21	0.78	0.55, 0.91
Wall volume	0.20	0.82	0.51, 0.95	0.20	0.84	0.63, 0.95	0.20	0.73	0.48, 0.92
Normalized wall index	0.10	0.74	0.42, 0.92	0.10	0.76	0.55, 0.91	0.10	0.68	0.41, 0.86
Mean wall thickness	0.11	0.68	0.39, 0.91	0.15	0.78	0.56, 0.92	0.13	0.73	0.49, 0.89

Note.—Inter- and intrareader estimates were based on readers reading 20 and 29 identical examinations, respectively (123 and 194 paired vessel segments, respectively), whereas examination estimates were based on readers reading 28 examination pairs (188 paired vessel segments). Measurements were over a fixed length for each vessel segment (supraclinoid internal carotid artery, 6 mm; M1 of middle cerebral artery, 6 mm; A1 of anterior cerebral artery, 6 mm; proximal and distal basilar artery, each 5 mm; and V4 of vertebral artery, 6 mm) and over the entire length of the largest plaque identified for each vascular territory. CI = confidence interval, CV = coefficient of variation, ICC = intraclass correlation coefficient.

Figure 2

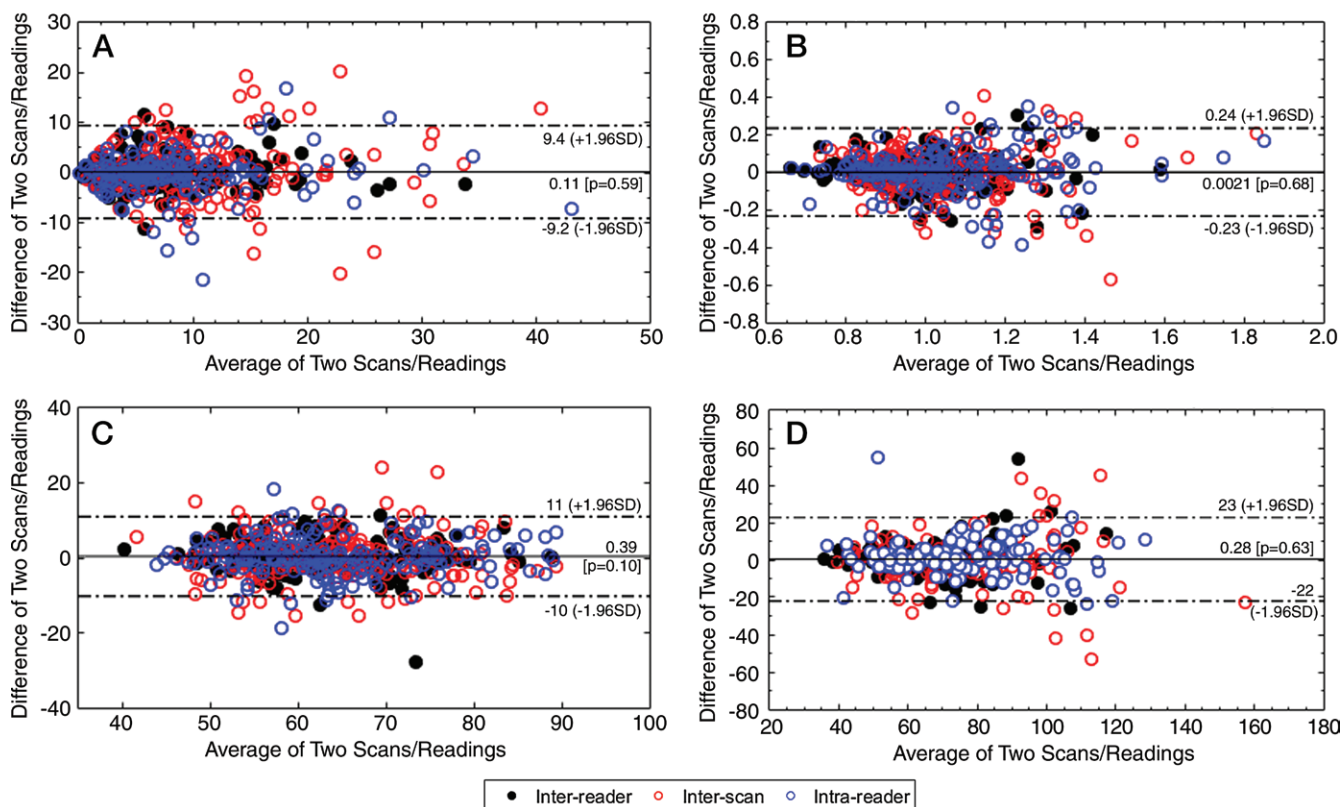


Figure 2: Bland-Altman plots for, A, diameter-based stenosis, B, mean wall thickness, C, normalized wall index, and, D, vessel volume. Solid lines indicate mean difference, and dashed lines indicate 95% limits of agreement. SD = standard deviation.

Vessel wall MR imaging has been used to identify and characterize ICAD in small-scale single-center studies

(7,8,17), but implementation in multiple centers presents additional challenges from variations in equipment and

performance of multiple MR imaging technologists and image analysts. With training, certification, and oversight

by our centralized MR imaging reading center, only 10.4% of participants were excluded because of inadequate QC scores despite the older age of this population. The 3D volume acquisition used herein simplifies the MR imaging protocol by including multiple intracranial vessels in one image, a considerable advantage over the 2D techniques typically used for ICAD imaging (10,18,19), which require identification of plaques during imaging and section positioning along inherently curving vessels. Wall thickness measurement error from partial volume averaging increases as image resolution exceeds wall thickness (10) and when anisotropic voxels are oriented oblique to the vessel axis, as is often encountered with 2D imaging of curved intracranial arteries (10,11). This offers an added advantage of 3D imaging, which acquires isotropic voxels at higher resolution than achievable with 2D techniques.

Estimates of reliability for black-blood MR imaging of ICAD have not been well established in the literature. Because our MR imaging technologists and image analysts were blinded to participant information, ensuring that repeat examinations could not be matched with baseline examinations, our reliability estimates are relevant to cross-sectional studies. Few previous studies have reported reader reliability estimates for black-blood MR imaging of ICAD (7,18–20), and most of these previous studies used 2D techniques; all previous studies included small sample sizes (18–20). Our current MR imaging technique reported herein offered good to excellent reliability for luminal and wall measurements of intracranial vessels and ICAD detection and likely can be used for planning sample size, quality control, and image analysis for future studies of ICAD.

We also provide population-based estimates of the frequency of ICAD according to age, sex, and race. The International Atherosclerosis Project (21), the largest autopsy study of atherosclerosis to date, demonstrated racial differences among African American and white participants. However, the results could not be generalized to

a living population (22). The Rotterdam study (23) reported that the prevalence of intracranial internal carotid artery calcifications in white European descendants was greater than 80%, although Mönckeberg arteriosclerosis accounts for calcifications in their study (24) and could overestimate the prevalence of atherosclerosis.

Limitations to our study include our inability to evaluate the accuracy of wall thickness measurements because no standard of reference for intracranial vessels exists. A limited report of intracranial wall thickness measurements based on a cadaver study (25) is not relatable because of the younger age of that population and the anticipated specimen shrinkage of up to 30% (26). However, our mean lumen area measurements agree with the results of published data (7,18–20). Resolution constraints limit our ability to stratify a narrow range of true wall thickness values, although this can be partly overcome with larger samples (27). All baseline and repeat examination pairs were obtained with the same imaging unit, so we could not estimate between-imager variation. However, all sites used Siemens platforms, and we expect this variation to be small.

In summary, we report the design and methods for the first population-based study to identify and quantify ICAD, offering new insight into its frequency and burden in the United States. Our MR imaging protocol characterized individuals at greatest risk for having ICAD lesions and offers a reliable technique for identifying lesions in patients suspected of having the disease.

Acknowledgments: The authors thank the staff and participants of the ARIC study for their important contributions.

Disclosures of Conflicts of Interest: Y.Q. Activities related to the present article: disclosed no relevant relationships. Activities not related to the present article: disclosed no relevant relationships. Other relationships: has a patent pending. E.G. disclosed no relevant relationships. F.K.S. disclosed no relevant relationships. L.L. disclosed no relevant relationships. Y.Z. disclosed no relevant relationships. Z.A. disclosed no relevant relationships. S.M. disclosed no relevant relationships. Y.J.X. disclosed no relevant relationships. N.N. disclosed no relevant

relationships. J.I. disclosed no relevant relationships. S.Z. disclosed no relevant relationships. A.A. disclosed no relevant relationships. H.C. disclosed no relevant relationships. D.C. disclosed no relevant relationships. B.A.W. Activities related to the present article: disclosed no relevant relationships. Activities not related to the present article: disclosed no relevant relationships. Other relationships: has a patent pending.

References

1. Wong LK. Global burden of intracranial atherosclerosis. *Int J Stroke* 2006;1(3):158–159.
2. White H, Boden-Albala B, Wang C, et al. Ischemic stroke subtype incidence among whites, blacks, and Hispanics: the Northern Manhattan Study. *Circulation* 2005;111(10):1327–1331.
3. Qureshi AI, Feldmann E, Gomez CR, et al. Consensus conference on intracranial atherosclerotic disease: rationale, methodology, and results. *J Neuroimaging* 2009;19(Suppl 1):1S–10S.
4. Bash S, Villablanca JP, Jahan R, et al. Intracranial vascular stenosis and occlusive disease: evaluation with CT angiography, MR angiography, and digital subtraction angiography. *AJNR Am J Neuroradiol* 2005;26(5):1012–1021.
5. Glagov S, Weisenberg E, Zarins CK, Stankunavicius R, Kolettis GJ. Compensatory enlargement of human atherosclerotic coronary arteries. *N Engl J Med* 1987;316(22):1371–1375.
6. Wasserman BA, Smith WI, Trout HH III, Cannon RO III, Balaban RS, Arai AE. Carotid artery atherosclerosis: in vivo morphologic characterization with gadolinium-enhanced double-oblique MR imaging initial results. *Radiology* 2002;223(2):566–573.
7. Qiao Y, Steinman DA, Qin Q, et al. Intracranial arterial wall imaging using three-dimensional high isotropic resolution black blood MRI at 3.0 Tesla. *J Magn Reson Imaging* 2011;34(1):22–30.
8. Qiao Y, Zeiler SR, Mirbagheri S, et al. Intracranial plaque enhancement in patients with cerebrovascular events on high-spatial-resolution MR images. *Radiology* 2014;271(2):534–542.
9. van der Kolk AG, Zwanenburg JJ, Brundel M, et al. Intracranial vessel wall imaging at 7.0-T MRI. *Stroke* 2011;42(9):2478–2484.
10. Wasserman BA, Astor BC, Sharrett AR, Swingen C, Catellier D. MRI measurements of carotid plaque in the atherosclerosis risk in communities (ARIC) study:

- methods, reliability and descriptive statistics. *J Magn Reson Imaging* 2010;31(2):406–415.
11. Antiga L, Wasserman BA, Steinman DA. On the overestimation of early wall thickening at the carotid bulb by black blood MRI, with implications for coronary and vulnerable plaque imaging. *Magn Reson Med* 2008;60(5):1020–1028.
 12. The Atherosclerosis Risk in Communities (ARIC) Study: design and objectives. The ARIC investigators. *Am J Epidemiol* 1989;129(4):687–702.
 13. Samuels OB, Joseph GJ, Lynn MJ, Smith HA, Chimowitz MI. A standardized method for measuring intracranial arterial stenosis. *AJNR Am J Neuroradiol* 2000;21(4):643–646.
 14. Suinesiaputra A, de Koning PJ, Zudilova-Seinsträ E, Reiber JH, van der Geest RJ. Automated quantification of carotid artery stenosis on contrast-enhanced MRA data using a deformable vascular tube model. *Int J Cardiovasc Imaging* 2012;28(6):1513–1524.
 15. Harris PA, Taylor R, Thielke R, Payne J, Gonzalez N, Conde JG. Research electronic data capture (REDCap): a metadata-driven methodology and workflow process for providing translational research informatics support. *J Biomed Inform* 2009;42(2):377–381.
 16. Fleiss J. *Statistical methods for rates and proportions*. 2nd ed. New York, NY: Wiley, 1981; 218.
 17. Swartz RH, Bhuta SS, Farb RI, et al. Intracranial arterial wall imaging using high-resolution 3-tesla contrast-enhanced MRI. *Neurology* 2009;72(7):627–634.
 18. Ryu CW, Jahng GH, Kim EJ, Choi WS, Yang DM. High resolution wall and lumen MRI of the middle cerebral arteries at 3 tesla. *Cerebrovasc Dis* 2009;27(5):433–442.
 19. Zhu XJ, Du B, Lou X, et al. Morphologic characteristics of atherosclerotic middle cerebral arteries on 3T high-resolution MRI. *AJNR Am J Neuroradiol* 2013;34(9):1717–1722.
 20. Li ML, Xu WH, Song L, et al. Atherosclerosis of middle cerebral artery: evaluation with high-resolution MR imaging at 3T. *Atherosclerosis* 2009;204(2):447–452.
 21. Solberg LA, McGarry PA. Cerebral atherosclerosis in persons with selected diseases. *Lab Invest* 1968;18(5):613–619.
 22. McMahan CA. Autopsied cases by age, sex, and “race”. *Lab Invest* 1968;18(5):468–478.
 23. Bos D, van der Rijk MJ, Geeraedts TE, et al. Intracranial carotid artery atherosclerosis: prevalence and risk factors in the general population. *Stroke* 2012;43(7):1878–1884.
 24. Fisher CM, Gore I, Okabe N, White PD. Calcification of the carotid siphon. *Circulation* 1965;32(4):538–548.
 25. Gutierrez J, Elkind MS, Petito C, Chung DY, Dwork AJ, Marshall RS. The contribution of HIV infection to intracranial arterial remodeling: a pilot study. *Neuropathology* 2013;33(3):256–263.
 26. Abramson DH, Scheffler AC, Almeida D, Folberg R. Optic nerve tissue shrinkage during pathologic processing after enucleation for retinoblastoma. *Arch Ophthalmol* 2003;121(1):73–75.
 27. Miao C, Chen S, Macedo R, et al. Positive remodeling of the coronary arteries detected by magnetic resonance imaging in an asymptomatic population: MESA (Multi-Ethnic Study of Atherosclerosis). *J Am Coll Cardiol* 2009;53(18):1708–1715.